NASA TECHNICAL NOTE

NASA TN D-4949

C.1

NASA TN D-4949

PREDICTIVE EQUATIONS FOR THERMAL NEUTRON FLUX PERTURBATION EFFECTS IN CYLINDERS

by John H. Lynch and Lawrence E. Peters, Jr.

Lewis Research Center
Cleveland, Ohio

NATIONAL AERONAUTICS AND SPACE ADMINISTRATION • WASHINGTON, D. C. • DECEMBER 1968

NASA TN D-4949

PREDICTIVE EQUATIONS FOR THERMAL NEUTRON FLUX PERTURBATION EFFECTS IN CYLINDERS

By John H. Lynch and Lawrence E. Peters, Jr.

Lewis Research Center
Cleveland, Ohio

NATIONAL AERONAUTICS AND SPACE ADMINISTRATION

For sale by the Clearinghouse for Federal Scientific and Technical Information
Springfield, Virginia 22151 – CFSTI price $3.00

ABSTRACT

The thermal-neutron flux perturbation, depression, and self-shielding factors were measured for several cylinders having different materials and dimensions. The measurements were done for the high-flux test positions of the Plum Brook Reactor. Results of these measurements were fitted to polynomials that can be used by designers of irradiation experiments to predict flux perturbation effects in test specimens. The experiment design, results, and uncertainty are discussed. The behavior of the perturbation factor around the experiment design center is also examined.

PREDICTIVE EQUATIONS FOR THERMAL NEUTRON FLUX PERTURBATION EFFECTS IN CYLINDERS

by John H. Lynch and Lawrence E. Peters, Jr.

Lewis Research Center

SUMMARY

In the design of irradiation experiments, prediction of the perturbation of the thermal-neutron flux by the experiment test specimens is frequently a problem. In order to obtain a model for calculating these perturbation effects, an experimental study was performed. A cylindrical shape was selected as being most typical of irradiation test specimens, and measurements of perturbation effects were made for several cylinders having different dimensions and made from different materials.

Regression analysis was used to obtain polynomials from these measurements. These polynomials can be used to predict the flux perturbation, depression, and self-shielding factors as functions of cylinder materials and dimensions and control rod position. These polynomials apply to the high-flux test positions. They can be used at other positions, but the accuracy there is unknown.

The polynomials cover a wide range of sizes and materials so that almost any cylindrical specimen that will fit into the high-flux test positions can be evaluated. In general, the error at the fitted points was only a few percent over the range of variables corresponding to most common materials and dimensions.

In many cases, the polynomials have several distinct advantages over numerical models or mockup measurements. They are general, and they are simple to use since they require no computer calculations or reactor time. Also, their uncertainty can be established quantitatively.

INTRODUCTION

Experimenters using the Plum Brook Test Reactor are initially provided with nominal measured and/or calculated unperturbed thermal flux distributions. They must adjust these to reflect the perturbation due to their experiments. The perturbed fluxes are

then used to compute such things as fission power and secondary gamma sources.

To determine the perturbing effect of an experiment, experimenters have used transport calculations when the perturbation has been large. And, if accurate knowledge of the perturbation factor is required for a successful experiment, mockup measurements are usually made. There are disadvantages associated with both of these practices. Nuclear mockups require design and fabrication, reactor scheduling, and data reduction. Numerical cell models are frequently unreliable because of their inherent misrepresentation of the neutron source and their geometrical inadequacies (e.g., selection of a transverse buckling in two-dimensional calculations can introduce considerable uncertainty for geometrically short regions). Even Monte-Carlo models can have arbitrary uncertainty unless a sufficient representation of the reactor as well as the irradiation capsule is used. And this type of calculation is frequently more expensive and time consuming to perform than a measurement.

The purpose of this study was to generate a set of equations that would enable an experimenter to calculate by hand the flux perturbation in his experiment. In order to be generally useful, the model had to apply to a variety of geometries and materials. It had to include any variable reactor parameters such as control-rod position and lattice location of the experiment. Also, the model had to be simple to use, and it had to yield reliable results. Reliability means, herein, that an experimenter could use this model with quantitative knowledge of the uncertainty in his calculated result. Because the results of preliminary calculations showed that the reliability objective would be difficult to meet with an analytical model, an experimental approach was adopted.

To obtain data that were generally applicable, a cylindrical shape was selected as representative of most irradiation test specimens (Thermionic diode fuel forms, mechanical test specimens, and reactor fuel-element rods are a few examples for which the perturbation factor in a cylinder is a significant problem). All other geometrical peculiarities such as sleeves, instrument leads, and mechanical support elements were ignored. These are usually not significant, and, in cases where they do affect the perturbation factor, their effects can usually be accounted for by corrections.

Perturbation, depression, and self-shielding factors were measured for several different cylinders, and the results were fitted to second-order polynomials. These polynomials act as mathematical french curves which relate the expected value of the response to the independent variables.

In this report the details of the experiment design and procedure are discussed. The resulting polynomial coefficients are presented, and the behavior of the perturbation factor polynomial around the center of the experiment design is examined.

SYMBOLS

$A_{n, nn}$	polynomial coefficient
C	blackness coefficient, ratio of net thermal-neutron current to thermal-neutron flux at cylinder surface
C^{jj}	diagonal elements of inverted sums of cross products deviations matrix
D	spatially averaged thermal-neutron flux depression factor
D_e	thermal-neutron diffusion coefficient in water at 68° F (293 K)
F	spatially averaged thermal-neutron-flux perturbation factor
H_{Cd}	elevation of bottom of cadmium in control rods
h_{cyl}	elevation of bottom of cylinder
J	subscript or superscript variable counter
K_J	first order, second order, or interaction variable in response equation
L	length of cylinder
N	number of experiments used to determine polynomial coefficients
Q	arbitrary variable denoting F, D, or SS
r	radius of cylinder
S	independent shadowing variable
SS	spatially averaged thermal-neutron-flux self-shielding factor
s	standard error of estimate (square root of residual variance)
t	student t
X_1	coded value of blackness coefficient, C (see eq. (8))
X_2	coded value of control-rod shadowing, S (see eq. (9))
X_3	coded value of cylinder length, L (see eq. (10))
β	albedo of cylinder
δ	coded independent variable level required for orthogonality
ϵ	extrapolation distance in grey cylinder of radius r
ϵ_b	extrapolation distance in black cylinder of radius r
λ_e	thermal-neutron transport mean free path in water at 68° F (273 K) (0.441 used)
Σ_a	thermal-neutron absorption cross section (for 2200 m/s neutrons)

Σ_{tr} thermal-neutron transport cross section

σ_Q standard error of Q polynomial

φ thermal-neutron flux with energy below cadmium cutoff

DESCRIPTION OF EXPERIMENT DESIGN

To extract the maximum amount of information from a minimum amount of data, an orthogonal[1] composite factorial experiment design was used (ref. 1). Details of this design are shown in appendix A. Observed data were perturbation, depression, and self-shielding factors. The number of independent variables was limited to three to keep the number of required experiments at a reasonable level without sacrificing accuracy in the fits and at the same time retaining the capability of seeing second-order and interaction effects. This meant that the choice of variables had to be made so that a strong dependence between the factors of interest and these selected variables was guaranteed.

The approach to the selection of variables was to first list the variables that were believed to affect the perturbation factor. Then this list was reduced by randomizing and combining variables where possible.

In order to account for the positive correlation between the scattering cross section and the perturbation factor and the negative correlation between the absorption cross section and the perturbation factor, these cross sections were combined with the radius into a single variable, the blackness coefficient C. This coefficient pertains to infinitely long cylinders; thus, the length L had to be retained as a separate variable.

The vertical position inside the hole and the rod position were replaced with one variable, the shadowing variable. This variable is the difference S between the elevation of the bottom of the cadmium in the control rod and the elevation of the bottom of the cylinder (see fig. 1).

Five values had to be selected for each of the three variables identified. These values correspond to the five experimental levels of ± 1.2154, ± 1.0, and 0 (see appendix A).

---

[1]After the data were obtained, a small nonorthogonality in one of the independent variables was discovered. The effect of this nonorthogonality was found to be negligible after the correlation coefficient matrices were examined. This problem was not present with the other two independent variables. They are at the orthogonal dimensions to within a few mils (mm).

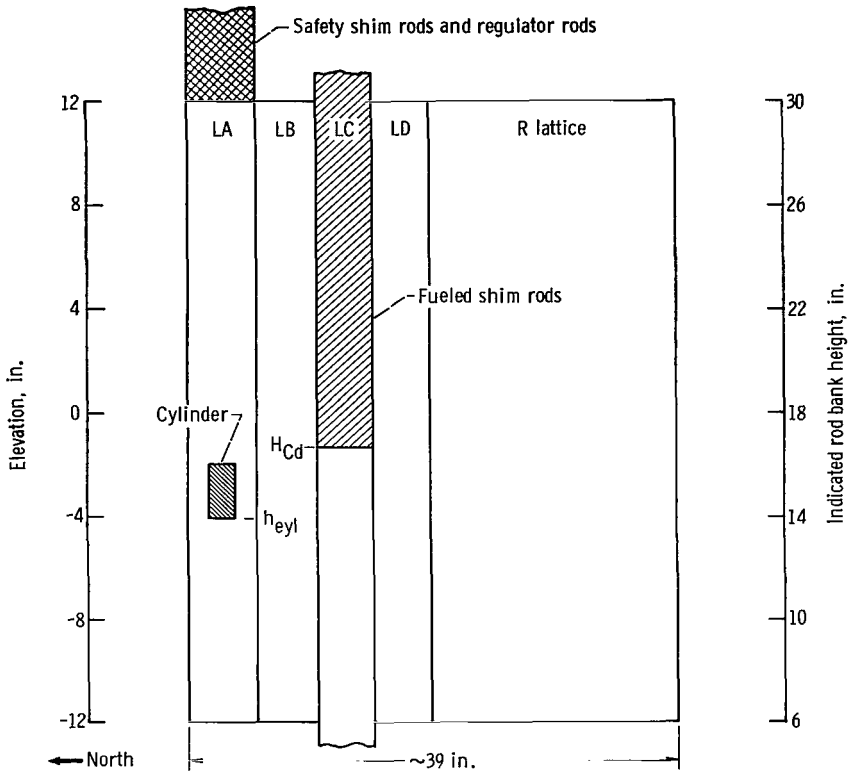

Figure 1. - Elevation view of Plum Brook core and reflectors showing relation among independent shadowing variable S, elevation of bottom of cadmium in control rods H_{Cd}, elevation of bottom of cylinder, and indicated rod bank position. For cylinder shown, $h_{cyl} = -4$ inches; $H_{Cd} = -1.325$ inches; $S = H_{Cd} - h_{cyl} = 2.675$ inches; indicated rod bank position, 16 inches.

Blackness, C. - The blackness coefficient is defined by

$$C \equiv \frac{D_e \varphi'(r)}{\varphi(r)} = \frac{D_e}{\epsilon} \tag{1}$$

where

$$D_e = \lambda_e/3 = \frac{\text{Transport mean free path in water}}{3} \tag{1a}$$

and

r cylinder radius

ϵ cylinder extrapolation distance

The extrapolation distance ϵ was obtained from Spinks' formula (ref. 2).

$$\frac{\epsilon}{\lambda_e} = \frac{\epsilon_b}{\lambda_e} + \frac{4(1 - \beta)}{3\beta} \tag{2}$$

where

$$\frac{\epsilon_b}{\lambda_e} = \frac{0.7140446 \frac{2r}{\lambda_e} + 1.080417}{\frac{2r}{\lambda_e} + 0.8103127} \tag{2a}$$

Four materials were selected for the cylinders. These were 304 stainless steel, cadmium, copper, and tungsten. These particular materials were selected (1) to give a good distribution in Σ_a, (2) to give a good representation of backscattering (some of the materials have a scattering cross section that is greater than the absorption cross section), and (3) to enable the complete range of possible blackness coefficients, for materials that will fit into one of the test positions, to be represented.

To select materials and radii for the various experiments, the following procedure was used. The computed blackness coefficients are based on the assumption that the cylinder is surrounded by water. For this assumption to be valid, there had to be some water surrounding every cylinder. The exact amount of water was somewhat arbitrary since the beryllium had some uncontrollable effect. The largest feasible cylinder was first selected arbitrarily as 1.5 inches in diameter. This left a 1/4-inch water annulus around the cylinder (because the experiment hole is about 2 inches in diameter (see fig. 2)).

The blackest 1.5-inch cylinder that could be put in a test position was cadmium (for which C is 0.4695). This was used to pick the other materials and sizes, but an undesirable distribution of radii resulted. Since it is not a great sacrifice in range of applicability to reduce this to a 1.0-inch diameter cadmium cylinder, this was done. This gave a maximum C value of 0.4236.

The lowest possible blackness limit is zero. This would require no experiment. However, the assumption of second-order behavior may have been invalid if zero were used. For this reason, the lower limit was arbitrarily selected as 0.04668 based on a stainless-steel cylinder having a radius of 0.4562 centimeter. The intermediate levels were then computed using these limits. A summary of the material properties (ref. 3) and radii is as follows:

Level	Material	Thermal-neutron absorption cross section, Σ_a	Scattering parameter, $1 - \Sigma_a/\Sigma_{tr}$	Blackness coefficient,[a] C	Radius, r, cm
-1.2154	304 stainless steel	0.2192	0.7757	0.04668	0.4562
-1.0000	Copper	.2889	.6497	.1211	1.000
0	Tungsten	1.0723	.2065	.2491	.715
1.0000	Cadmium	131.33	.0028	.3873	.560
1.2154	Cadmium	131.33	.0028	.4236	1.2700

[a]This variable is not quite orthogonal. The effect of this nonorthogonality was found to be negligible.

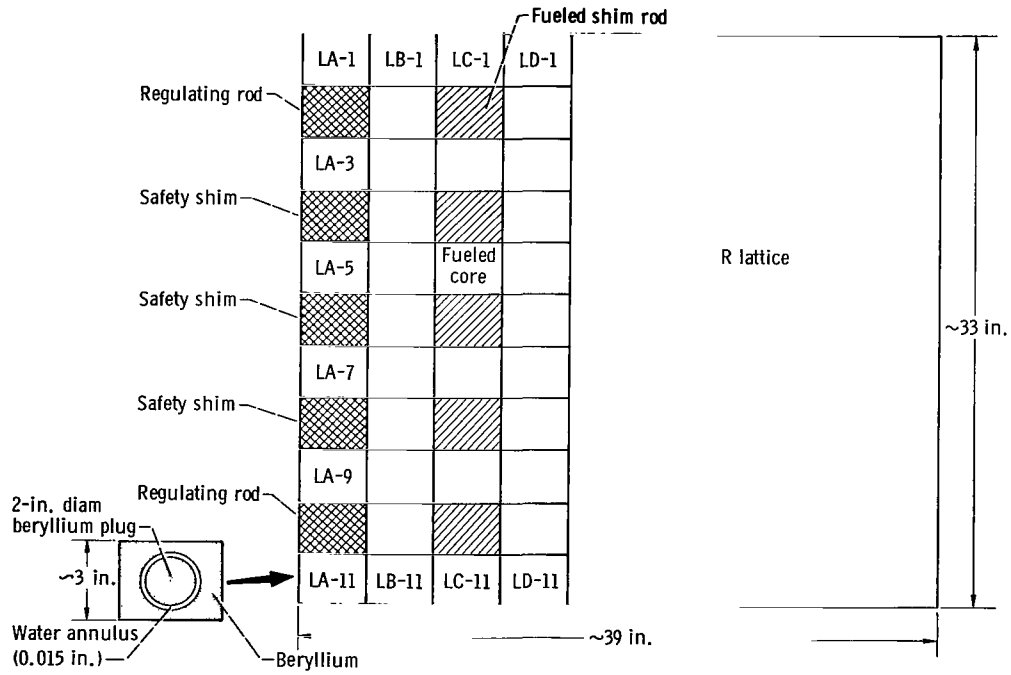

Figure 2. - Plan view of Plum Brook reactor core and reflectors showing lattice positions. The L-pieces (LA-1, LB-1, etc.) and R lattice are about 10 percent water and 90 percent beryllium. When making perturbation measurement, beryllium plug is removed and cylinder is placed in water-filled hole.

Control rod shadowing S. - Control rod shadowing is the difference between the elevations of the cylinder bottom and the cadmium bottom ($S \equiv H_{Cd} - h_{cyl}$). To establish values, the practical range of rod motion was considered (positions of 16 and 28 in.; see fig. 1). Placing the shortest cylinder (2.54 cm) at extreme ends (vertically) of the core gave ±1.2154 level values of S when the rods are in the extreme position. This gave -31.3, -23.5, ±13.1, 49.7, and 57.5 centimeters for the five required levels of S.

Length, L. - The shortest length was arbitrarily selected as 2.54 centimeters. The longest was selected as 15.24 centimeters. This made the zero value 8.89 centimeters, and the plus and minus 1.0 levels 14.11 and 3.67 centimeters, respectively.

Miscellaneous. - The lattice position (see fig. 2) is a qualitative rather than a quantitative factor and the two cannot be easily mixed. Hence, it was randomized so that the effect it produced on the results was not systematic. The lattice position effect is thus confounded with the regression polynomial coefficients. The polynomials thus represent any lattice position. It was assumed, also, that the lattice position effect was small. This assumption was found to be justified after the experimental data were obtained. The ratio of explained to unexplained variance was at least 0.99 for the perturbation, depression, and self-shielding factors.

EXPERIMENTAL TECHNIQUE

The perturbation, self-shielding, and depression factors for a given cylinder were determined by measuring the thermal neutron flux at various points on the surface and inside the cylinder. These thermal flux values were then numerically integrated over the cylinder volumes or surface. The integrals of the fluxes over Lucite cylinders of the same size were also determined, and the ratio of these two integrals (see section RESULTS AND DISCUSSION) was used to obtain the perturbation, self-shielding, and depression factors for the cylinder.

Thermal flux values were obtained by activation analysis of gold wires. Activation due to epicadmium neutrons, determined by placing cadmium-covered gold wires at several positions in and on the cylinders, was subtracted from bare gold activity to give the activity due to the thermal flux alone. The flux depression effect due to the gold detectors and the cadmium covers was taken into account by using the same number of gold detectors and cadmium covers in and on the Lucite cylinder and by locating them symmetric to the detector locations in the metal cylinder. Thus, the flux in the unperturbed cylinder would be subject to the same inherent depression, because of the flux monitors, as in the metal cylinder.

Figure 3 shows a typical cylinder and Lucite mockup and the rig used for positioning the cylinders in the test holes. The small holes in the cylinders are for 0.5-inch long by 0.030-inch diameter gold flux wires. The telescoping section on the bottom of the positioning rig enables exact vertical positioning of the cylinder in the core lattice hole.

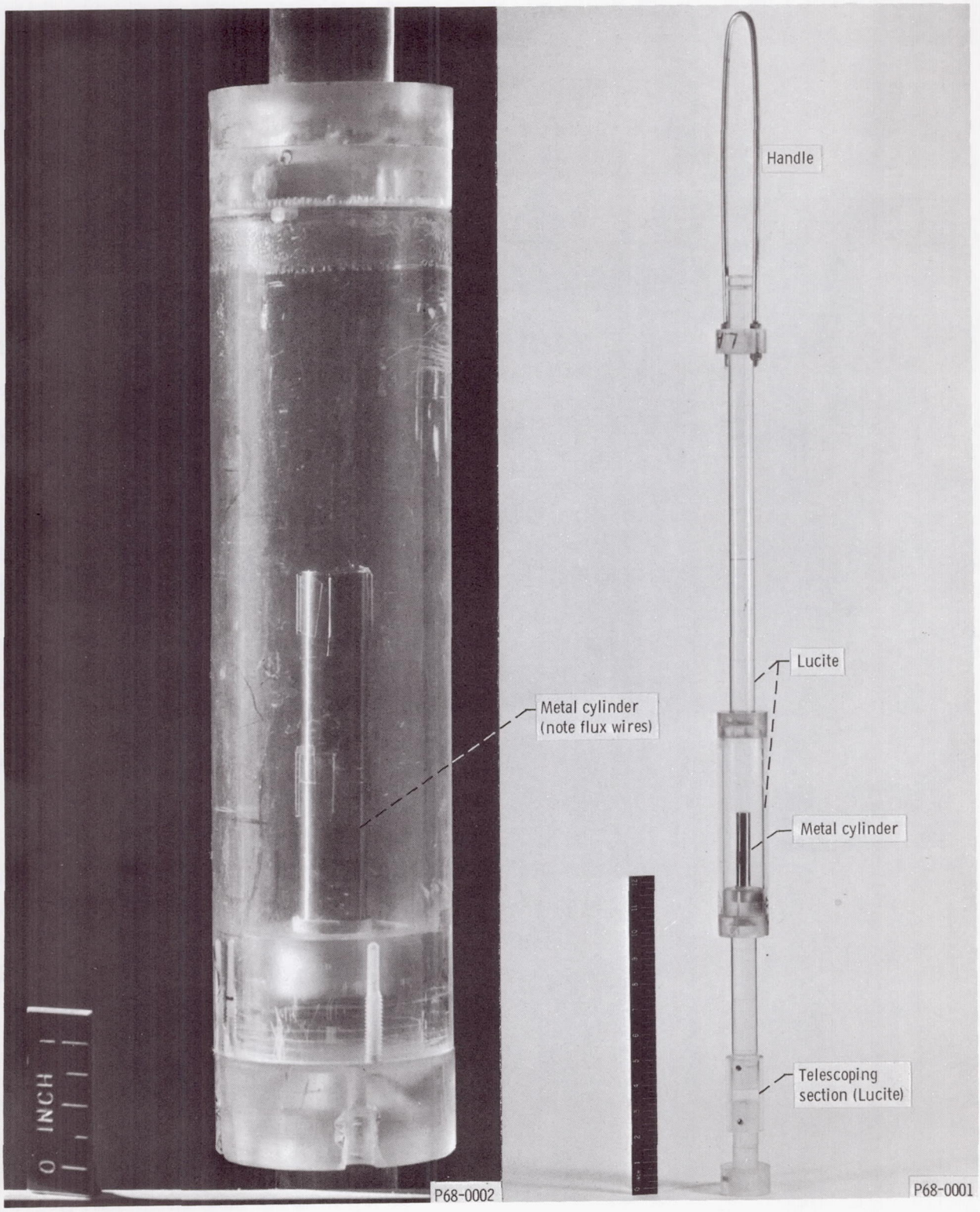

(a) Cylinder positioning rig.

Figure 3. - Apparatus.

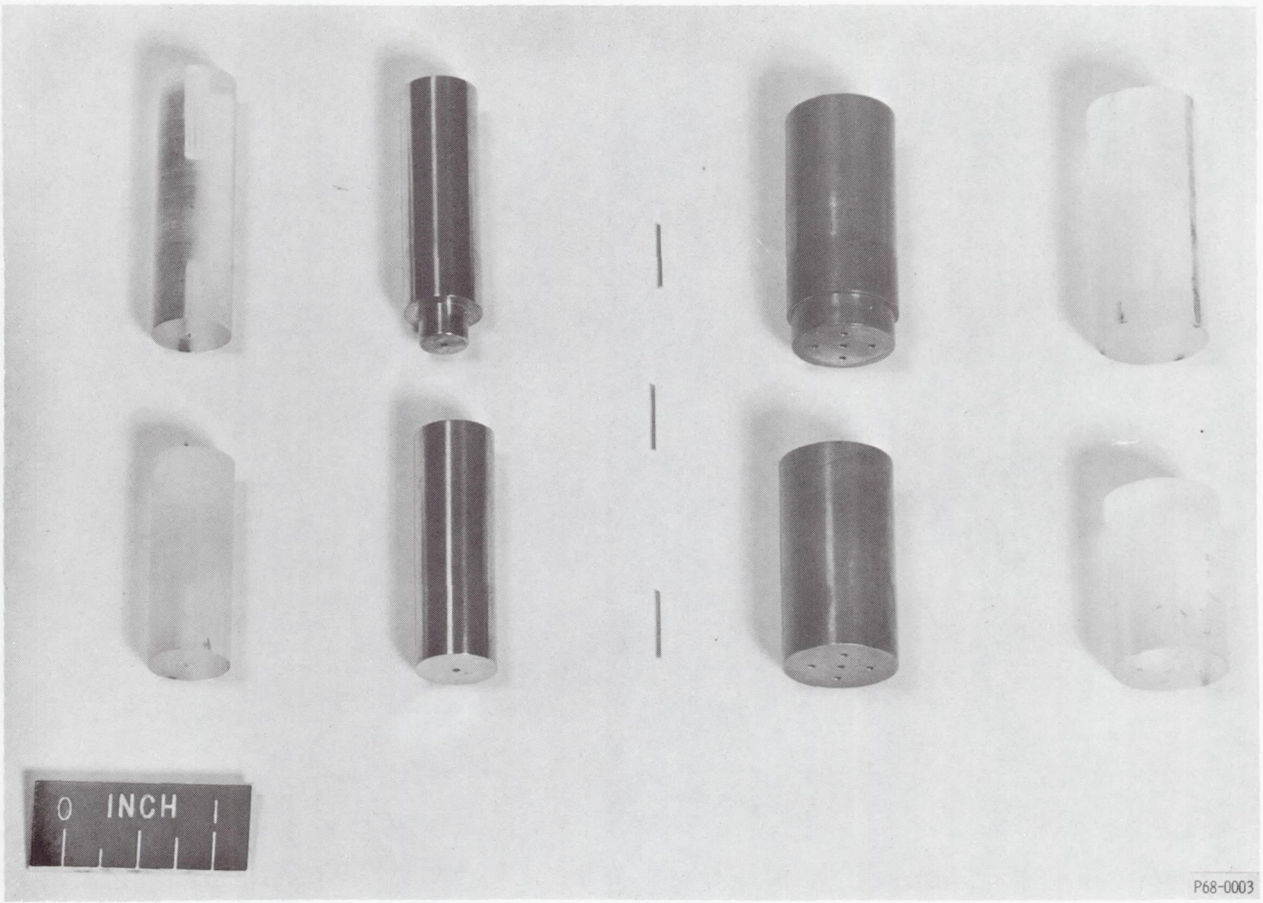

(b) Typical metal and lucite cylinders.

Figure 3. - Concluded.

Figure 2 is a plan view of the reactor core showing the lattice positions where the measurements were made. For a given measurement, the rig with the metal cylinder would be placed in a specified lattice position, for example, LA-3; then a similar positioning rig with the Lucite mockup cylinder would be placed in the symmetric lattice position, for example, LA-9, to obtain the unperturbed flux. This method relies on the established flux symmetry of the reactor and avoids errors due to power normalization.

There was negligible probability of systematic error due to interaction between holes because the cylinders used in adjacent holes LA-3 and LA-5 (where this might have been a problem) were small. This was not by design but occurred when the lattice positions were randomly selected.

For the cylinders not made of cadmium, at least one foil of each axial tier was cadmium-covered to allow correction for spatial variation of the cadmium ratio. Also, for the cylinders that were not made of cadmium, the flux radially across the cylinders was not greatly perturbed. Thus, the particular method used for numerical integration was not important. The data were analyzed using several different weighing methods. Essentially the same results were obtained.

The cadmium cylinders presented a special problem in that any dosimeters inside the cylinder would measure relatively low thermal fluxes. An attempt was made to measure the normal gradients at the cylinder surface and to infer the volume integrated fluxes; this, however, proved to be an unreliable method. The gradients were underestimated because of the finite distance that had to be maintained between foils. We chose instead to infer the perturbation factor for the cadmium using the computed blackness coefficients and the integrals of the surface fluxes. For the cadmium cylinders, the average flux in the cylinders was defined by

$$\varphi_{Cd} \equiv \frac{C \int \varphi \, dS}{\Sigma_a \int dv} \tag{3}$$

RESULTS AND DISCUSSION

The perturbation factor F is defined as

$$F \equiv \frac{\int_{\substack{\text{Metal} \\ \text{cylinder}}} \varphi_{th} \, dv}{\int_{\substack{\text{Lucite} \\ \text{cylinder}}} \varphi_{th} \, dV} \tag{4}$$

The flux depression factor D is defined as

$$D \equiv \frac{\int_{\substack{\text{Metal} \\ \text{cylinder}}} \varphi_{th}\, dS}{\int_{\substack{\text{Lucite} \\ \text{cylinder}}} \varphi_{th}\, dS} \tag{5}$$

The self-shielding factor SS is defined as the ratio of perturbation to depression factors

$$SS \equiv \frac{F}{D} \tag{6}$$

In the preceeding equations, φ_{th} is the subcadmium gold activity and dS and dV refer to surface and volume integration.

The ranges of variables studied were from 0.04668 to 0.4236 for the blackness coefficient, from 2.54 to 15.24 centimeter for the cylinder lengths and from -31.3 to 57.5 centimeters for the control-rod shadowing variable.

Polynomials were obtained for the perturbation factor F, the flux depression factor D, and the self-shielding factor SS. Two types of fit were made for each factor. One type used the coded form of the independent variables, and the other type used the uncoded values. The calculations for the fitting showed poor matrix conditioning when the uncoded data were used. The polynomials for the uncoded data were thus much more sensitive to small errors in the independent variables. For this reason, only the polynomials that use coded data will be discussed.

The form of the response polynomials is

$$\begin{aligned}\arcsin(Q^{1/2}) = {} & A_0 + A_1X_1 + A_2X_2 + A_3X_3 + A_{11}X_1^2 + A_{22}X_2^2 \\ & + A_{33}X_3^2 + A_{12}X_1X_2 + A_{13}X_1X_3 + A_{23}X_3X_2\end{aligned} \tag{7}$$

where Q is the flux perturbation, depression, or self-shielding factor and X_1, X_2, and X_3 are coded independent variables defined by

$$X_1 \equiv \frac{C - 0.2491}{0.2491 - 0.1211} \tag{8}$$

$$X_2 \equiv \frac{S - 13.1}{49.7 - 13.1} \tag{9}$$

and

$$X_3 \equiv \frac{L - 8.89}{14.11 - 8.89} \tag{10}$$

The polynomial coefficients, obtained by least squares fitting (ref. 4) are shown in table I.

TABLE I. - POLYNOMIAL COEFFICIENTS FOR EQUATION (7)

Coefficient	Spatially averaged thermal-neutron flux factors for -		
	Perturbation, F	Depression, D	Self-shielding, SS
A_0	0.748233	0.720736	1.323520
A_1	-.381871	-.169878	-.524997
A_2	-.001188	-.001071	.002519
A_3	-.028967	-.030870	-.025436
A_{11}	-.107360	.038095	-.314288
A_{22}	-.072745	.006349	-.123187
A_{33}	-.071242	.015803	-.142835
A_{12}	.001099	.002913	.000007
A_{13}	.021371	.004981	.017675
A_{23}	.001144	.003210	.000066

Use of the arc sin transformation makes the variance in the fit independent of the actual values of the data points and dependent only on the number of data points (ref. 5). This is a common transformation for data that vary between zero and one. It gave much better agreement at the measured points than several others that were tried. Among those rejected were $\log_e(F)$, F, and $\log_e X_1$.

Table II is a comparison of the measured F, D, and SS values and the polynomial approximations of these values. The percent error at each point and statistical measures of accuracy are also given. The error at the experimental points provides a first-order estimate of the error that can be expected for intermediate points calculated using the polynomials (see experiments 16 and 17 in table II). The statistical measures of fit tend to verify the selection of variables and to provide some indication of the overall error and dispersion in the fits. If a more exact estimate of the uncertainty is desired,

TABLE II. - SUMMARY OF POLYNOMIAL ACCURACY

Experiment	Coded values			Spatially averaged thermal-neutron flux factors								
				Perturbation, F			Depression, D			Self-shielding, SS		
	Blackness coefficient, X_1	Control-rod shadowing, X_2	Cylinder length, X_3	Measured value	Polynomial approximation	Error, percent	Measured value	Polynomial approximation	Error, percent	Measured value	Polynomial approximation	Error,[a] percent
1	$-\delta$	0	0	0.807	0.781	-3.2	0.832	0.786	-5.5	0.970	0.958	-1.2
2	-1	-1	-1	.623	.645	3.5	.675	.695	3.0	.923	.932	.1
3	-1	-1	1	.524	.544	3.8	.598	.630	5.3	.876	.886	1.1
4	-1	1	-1	.618	.638	3.2	.668	.692	3.6	.925	.929	.4
5	-1	1	1	.524	.542	3.4	.598	.630	5.3	.876	.881	.6
6	0	$-\delta$	0	.397	.358	-9.8	.462	.446	-3.5	.859	.816	-5.0
7	0	0	$-\delta$	.434	.394	-9.2	.498	.496	-.4	.871	.825	-5.3
8	0	0	0	.380	.465	22.3	.441	.434	-1.6	.862	.940	9.0
9	0	0	δ	.356	.326	-8.4	.438	.423	-3.4	.813	.778	-4.3
10	0	δ	0	.388	.356	-8.2	.446	.442	-.9	.870	.831	-4.5
11	1	-1	-1	.00423	.00536	26.8	.370	.349	-5.7	.0114	.0165	44.8
12	1	-1	1	.00292	.00356	18.0	.309	.297	-3.9	.00945	.0133	40.7
13	1	1	-1	.00421	.00511	21.3	.369	.346	-6.2	.0114	.0177	55.2
14	1	1	1	.00335	.00385	13.0	.325	.304	-6.4	.0103	.0145	40.7
15	δ	0	0	.00117	.000790	-32.5	.214	.282	31.7	.00547	.00059	-90.7
[b]16	-1.45	0.833	-0.243	0.652	0.745	14.3	0.678	0.750	10.6	0.962	0.920	-4.4
[b]17	-1.24	.833	1	.596	.600	.7	.651	.685	5.2	.916	.885	-3.4

[a]Percent difference may be misleading for experiment 15. The ratio of measured to polynomial values is 10.

[b]These extra measurements were made to test the fits at points not used in determining the polynomial coefficients.

the 95-percent confidence interval associated with equation (7) may be computed as shown in appendix B.

The average absolute error in the fitted F values (excluding experiments 16 and 17) is 12.2 percent. In the range of most interest (first 10 measurements), the error is only 7.0 percent. In this range, the average absolute error in SS is 3.2 percent.

The behavior of the perturbation factor F around the experiment design center is shown in figures 4 to 6. Note in figure 5 that, although the F polynomial behavior is reasonable at the nominal blackness and shadowing, the trend is misrepresented by the polynomial below a length of about 9 centimeters. This is a peculiarity of the fit. The center value can be seen from the tabulated comparison of errors to be much more poorly fit than values to either side of it. The trend of decreasing F with increasing L is correctly represented away from the design center. This can be seen from experiments 2 and 3 and, also, 13 and 14. Similar observations can be made about the shadowing variable (fig. 6). These anomalies could possibly have been reduced by replicating the center point but, since the polynomials have acceptable accuracy, this was felt unnecessary.

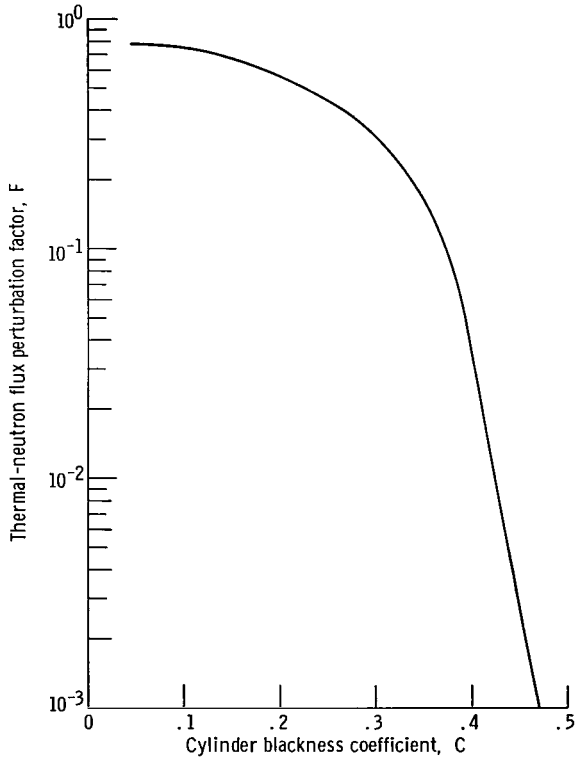

Figure 4. - Thermal flux perturbation factor as function of cylinder blackness coefficient. Cylinder length, 8.89 centimeters; shadowing, 13.1 centimeters.

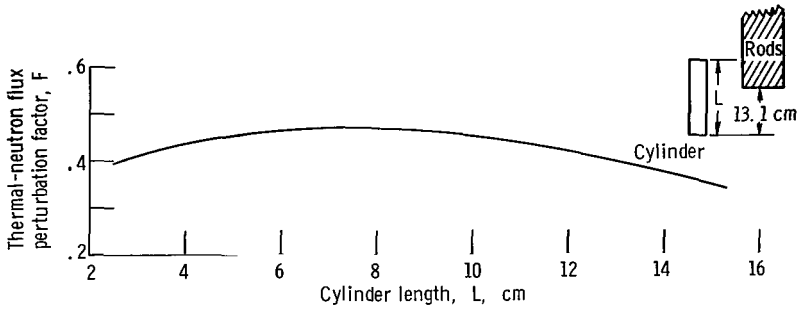

Figure 5. - Thermal flux perturbation factor as function of cylinder length. Blackness coefficient, 0.23; shadowing, 13.1 centimeters.

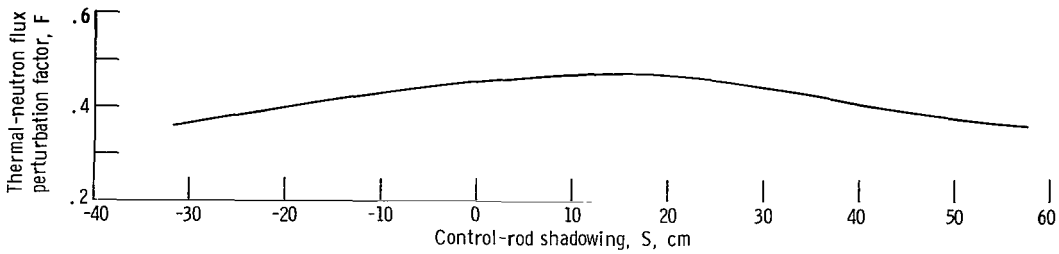

Figure 6. - Thermal-neutron flux perturbation factor as function of control-rod shadowing for cylinder length. 8.89 centimeters; blackness coefficient, 0.23.

The regression models do not distinguish radius from Σ_{tr} because these variables are multiplied together when C is determined. Also, the effects of the core vertical fuel termination near the top and bottom of the core are not accounted for by the S variable. The S variable assumes that the core is infinitely high. Based on the agreement at the measured points, however, these effects appear not to be important.

All the error analyses discussed herein refer to errors in the fits. No mention has been made of the errors in the flux measurements. This kind of error is difficult to evaluate because of the finite integration and ratios used in generating the perturbation, self-shielding, and depression factors. The uncertainty (due to counting) in the measured flux at a point is less than 2 percent. Since both perturbed and unperturbed fluxes were measured simultaneously in the same reactor run, no power normalization error was incurred. Symmetric lattice positions were used for perturbed and unperturbed measurements, and symmetric foil positioning and cylinder orientation as well as cadmium cover positioning also tended to keep the experimental error very small. A reasonable estimate is less than 5 percent.

CONCLUDING REMARKS

The polynomials derived from this work enable convenient hand calculations of flux perturbation effects in cylinders in water-filled Plum Brook reactor test holes. This is a specialization of the perturbation problem and does not apply exactly to any specific irradiation test specimen. Effects of specimen holders, cladding, etc., must be treated separately. This requires some judgement on the part of the designer as to how well his specimen is represented by a cylinder in water. The polynomial model only attempts to represent the salient features of the problem, namely, the slowing source, exponential flux gradient across the specimen, specimen geometry (to first order), specimen material, and control-rod shadowing effects. For experiments closely resembling cylinders, the polynomials will give accurate results. For experiments having significant differences from the simple cylinder model, the polynomials, suitably corrected, should provide a useful tool in initial design and survey studies.

For cases in which the polynomials can be applied directly or with minor corrections, they have several distinct advantages over numerical models or mockup measurements. They are general and simple to use because they require no computer calculations or reactor time. Also, their uncertainty can be established quantitatively.

Lewis Research Center,
National Aeronautics and Space Administration,
Cleveland, Ohio, September 24, 1968,
120-27-04-54-22.

APPENDIX A

DETAILS OF ORTHOGONAL COMPOSITE DESIGN

To generate the response polynomials, 15 measurements were performed. Each measurement included a perturbed and an unperturbed integrated thermal flux for the cylinder of interest. The statistical experiment design was an orthogonal composite fractional factorial. Levels of independent variables for each of the experiments are shown in sketch (a):

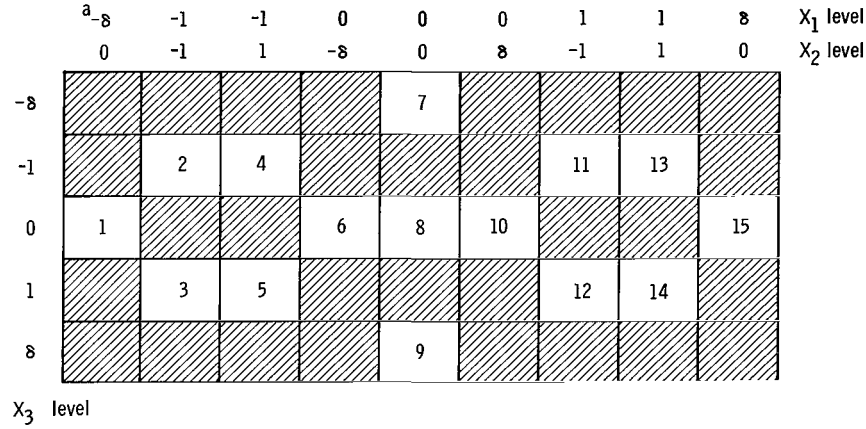

[a]δ is the value of the highest and lowest levels; δ = 1.2154 for orthogonality. Numbers in blocks are experiment numbers, 1.

(a)

The blackness coefficient C (variable X_1) was slightly off orthogonal. The effect of this slight nonorthogonality was found to be negligible by inspecting the correlation coefficient matrix. The exact levels used for this variable are shown in another section. The orthogonal design was selected to increase the accuracy of the response equations.

The sketch shows the levels of each of the independent variables used in each of the 15 experiment sets. For example, experiment 1 has the $-\delta$ of X_1, the zero level of X_2, and the zero level of X_3. Equations (8) to (10) define X_1, X_2, and X_3.

APPENDIX B

CONFIDENCE LIMITS FOR POLYNOMIALS

Given any of the predictive polynomials

$$\text{arc sin } Q^{1/2} = \text{arc sin } Q^{1/2}(K_1, K_2, \ldots, K_j) \tag{B1}$$

where the K_j are first order, second order, or interaction variables, the variance in the computed arc sin $Q^{1/2}$ is given by

$$\sigma_Q^2 = s^2\left[\frac{1}{N} + C^{11}(K_1 - \overline{K}_1)^2 + \ldots + C^{jj}(K_j - \overline{K}_j)^2 + 2C^{12}(K_1 - \overline{K}_1)(K_2 - \overline{K}_2) + \ldots\right] \tag{B2}$$

where

N number of measurements, 15

C elements of inverted sums-of-cross-products-deviations matrix

K_j independent variable (X_1, X_1^2, X_1X_2, etc) in response polynomial

$\overline{K}_j$ mean value of j^{th} independent variable

s^2 residual variance

Since the design is nearly orthogonal, the covariances (terms multiplied by 2 in eq. (B2)) can be neglected. Also, the design is balanced around zero so that all the $\overline{K}_j$ are zero.

This gives for the standard error in arc sin $Q^{1/2}$

$$\sigma_Q \approx s\left[\frac{1}{N} + \sum_{j=1}^{9} C^{jj}K_j^2\right]^{1/2} \tag{B3}$$

For the perturbation factor, this is

$$\sigma_F \approx 0.0564\left[0.0667 + 0.0771\,X_1^2 + 0.0914\,X_2^2 + 0.0914\,X_3^2 + 0.1333\,X_1^4 + 0.2343\,X_2^4 + 0.2343\,X_3^4 + 0.1156\,X_1^2X_2^2 + 0.1156\,X_1^2X_3^2 + 0.1250\,X_2^2X_3^2\right]^{1/2} \tag{B4}$$

For the depression factor, it becomes

$$\sigma_D \approx 0.0569\left[0.0667 + 0.0771\,X_1^2 + 0.0914\,X_2^2 + 0.0914\,X_3^2 + 0.1333\,X_1^4 + 0.2351\,X_2^4 + 0.2339\,X_3^4 + 0.1156\,X_1^2X_2^2 + 0.1156\,X_1^2X_3^2 + 1250\,X_2^2X_3^2\right]^{1/2} \quad \text{(B5)}$$

and, for the self-shielding factor,

$$\sigma_{SS} \approx 0.0837\left[0.0667 + 0.0771\,X_1^2 + 0.0915\,X_2^2 + 0.0913\,X_3^2 + 0.1333\,X_1^4 + 0.2351\,X_2^4 + 0.2339\,X_3^4 + 0.1156\,X_1^2X_2^2 + 0.1156\,X_1^2X_3^2 + 1250\,X_2^2X_3^2\right]^{1/2} \quad \text{(B6)}$$

must be used. The constants in these equations were computed when the polynomial coefficients were obtained.

The confidence intervals are given by

$$(\text{Confidence limits})_Q = \text{arc sin } Q^{1/2} \pm t\sigma_Q \quad \text{(B7)}$$

and 2.57 is the two-sides student t for 95 percent confidence with five degrees of freedom.

REFERENCES

1. Davies, O. L., ed.: The Design and Analysis of Industrial Experiments. Second ed., Hafner Publishing Company, 1956.

2. Spinks, N.: The Extrapolation Distance at the Surface of a Grey Cylindrical Control Rod. Nucl. Sci. Eng., vol. 22, no. 1, May 1965, pp. 87-93.

3. Anon.: Reactor Physics Constants. Rep. ANL-5800, second ed., Argonne National Lab., July 1963.

4. Draper, N. R.; and Smith, H.: Applied Regression Analysis. John Wiley & Sons, Inc., 1966.

5. Mosteller, F.; and Tukey, J. W.: The Uses and Usefulness of Binomial Probability Paper. Am. Stat. Assoc. J., vol. 44, June 1949, pp. 174-212.

NASA-Langley, 1968 — 22 E-4614

NATIONAL AERONAUTICS AND SPACE ADMINISTRATION
WASHINGTON, D. C. 20546

OFFICIAL BUSINESS

FIRST CLASS MAIL

POSTAGE AND FEES PAID
NATIONAL AERONAUTICS AND
SPACE ADMINISTRATION

POSTMASTER: If Undeliverable (Section 158 Postal Manual) Do Not Return

"The aeronautical and space activities of the United States shall be conducted so as to contribute . . . to the expansion of human knowledge of phenomena in the atmosphere and space. The Administration shall provide for the widest practicable and appropriate dissemination of information concerning its activities and the results thereof."

—NATIONAL AERONAUTICS AND SPACE ACT OF 1958

NASA SCIENTIFIC AND TECHNICAL PUBLICATIONS

TECHNICAL REPORTS: Scientific and technical information considered important, complete, and a lasting contribution to existing knowledge.

TECHNICAL NOTES: Information less broad in scope but nevertheless of importance as a contribution to existing knowledge.

TECHNICAL MEMORANDUMS: Information receiving limited distribution because of preliminary data, security classification, or other reasons.

CONTRACTOR REPORTS: Scientific and technical information generated under a NASA contract or grant and considered an important contribution to existing knowledge.

TECHNICAL TRANSLATIONS: Information published in a foreign language considered to merit NASA distribution in English.

SPECIAL PUBLICATIONS: Information derived from or of value to NASA activities. Publications include conference proceedings, monographs, data compilations, handbooks, sourcebooks, and special bibliographies.

TECHNOLOGY UTILIZATION PUBLICATIONS: Information on technology used by NASA that may be of particular interest in commercial and other non-aerospace applications. Publications include Tech Briefs, Technology Utilization Reports and Notes, and Technology Surveys.

Details on the availability of these publications may be obtained from:

SCIENTIFIC AND TECHNICAL INFORMATION DIVISION

NATIONAL AERONAUTICS AND SPACE ADMINISTRATION

Washington, D.C. 20546